ELSEVIER

Diamond and Related Materials 5 (1996) 1012–1016

DIAMOND AND RELATED MATERIALS

Structural limitations to local thermal diffusivities of diamond films [1]

H. Verhoeven [a], J. Hartmann [b], M. Reichling [b], W. Müller-Sebert [c], R. Zachai [a]

[a] *Daimler-Benz AG, Materials Research, D-89013 Ulm, Germany*
[b] *Freie Universität Berlin, Fachbereich Physik, Arnimallee 14, D-14195 Berlin, Germany*
[c] *Fraunhofer-Institut für Angewandte Festkörperphysik, Tullastrasse 72, D-79108 Freiburg, Germany*

Received 10 September 1995

Abstract

The photothermal displacement technique at transient thermal gratings and photothermal microscopy, both providing a spatial resolution on a micrometer scale, were used to investigate the thermal properties of crystallites and regions located between crystallites of diamond grown by microwave plasma chemical vapour deposition. The thermal properties are related to the structural properties by micro-Raman/photoluminescence spectroscopy and infrared spectroscopy. In the vicinity of a highly defective region located between crystallites, which exhibits a preferential incorporation of non-diamond carbon, silicon-vacancy complexes and hydrogen, a reduction of the thermal diffusivity by about 35% was observed. Depending upon whether this region is a grain boundary or a defect-filled microcrack, the decrease in the thermal diffusivity is caused by enhanced phonon scattering from these defects accumulated at the boundary or by a vanishing transmission probability of phonons across the crack. High thermal conductivities between 1500 W $m^{-1}K^{-1}$ and 1700 W $m^{-1}K^{-1}$ were determined within the crystallites at room temperature.

Keywords: Thermal properties; Structural properties; Microstructure

1. Introduction

The unusual combination of high thermal conductivity and low electrical conductivity makes diamond a promising material for heat-spreading applications in high-power electronic devices. Diamond films fabricated using chemical vapour deposition (CVD) offer the potential of inexpensive and device-adapted solutions for thermal problems, such as direct deposition of diamond on electronic devices. This method avoids the thermal resistance induced by interfacial bonding materials required for the attachment of high thermal conductivity diamond plates to the devices, but the inferior thermal properties of the interface layer due to the polycrystalline and columnar structure of CVD diamond films acts as an effective thermal barrier. For a further improvement in the performance for thermal management applications, it is of fundamental interest to understand the limitations to the heat conduction properties of CVD diamond due to its microscopic structure. Recent research has modelled both vertical and lateral thermal conductivities in dependence on the grain size with the assumption that all point and extended defects are concentrated at the grain boundaries with a fixed number of defects per unit area of grain boundary [1,2]. However, there is a lack of experimental investigations on a laterally local scale, since most thermal methods measure integrated thermal conductivities of diamond in a macroscopic manner for all or a large portion of the sample.

In this work we report on two microscopic, thermal mapping experiments over crystallites and regions located between crystallites of CVD diamond using the photothermal displacement technique at transient thermal gratings and photothermal microscopy. The former method enables the determination of lateral thermal diffusivities with a spatial resolution of about 20 μm, while the latter yields information about thermal properties with a spatial resolution of several micrometers depending on the modulation frequency and the thermal conductivity of the crystallite. In order to correlate the observed thermal diffusivity behaviour directly with the structural properties of the film, micro-Raman, micro-photoluminescence and infrared spectroscopy measurements were carried out.

[1] Paper presented at the 6th European Conference on Diamond, Diamond-like and Related Materials, Barcelona, 10–15 September 1995.

SSDI 0925-9635(95)00489-0

2. Experimental details

The investigated diamond sample with a thickness of 170 μm was grown by standard microwave-plasma-assisted CVD on a silicon substrate. For facilitating photothermal and infrared transmission investigations, the growth surface was polished and the substrate removed.

The thermal characterization of the CVD diamond film was first performed with the transient thermal grating technique. A detailed description of the method is given in Ref.[3]. Briefly, this method is based on surface heating by absorbing laser light from a pulsed Nd:YAG-laser producing a well-defined interference pattern. The surface displacement due to thermal expansion is measured by the angular deflection of a strongly focused He–Ne laser beam reflected from the surface. The analysis of the measured transient surface displacement decay yields the lateral thermal diffusivity of the sample within a thermal diffusion length of $L_{th} = (\Lambda/\pi)$, which is governed by the grating period Λ of the interference pattern. Thus, typical grating periods between 60 and 150 μm result in a spatial resolution of some tens of micrometers, which facilitates investigations of the microscopic structural limitations to thermal diffusivities of polycrystalline CVD diamond films [4]. Because of the high optical transmission of the diamond samples, sputtered Cr films about 30 nm thick are deposited on the surface of the samples in order to enhance the laser absorption without affecting the thermal properties. Signal averaging over about 600 laser pulses yields a signal-to-noise ratio of about 20 for diamond films and an uncertainty of ±10% for each measurement.

The interesting features seen in the thermal grating measurements were further investigated with the photothermal microscope at room temperature. A description of this technique can be found in Ref.[5]. In principle, this method measures the temperature at the sample surface, heated by a modulated highly focused Ar^+-ion laser spot with a 1/e radius of about 1 μm, via a He–Ne laser probe beam of the same size, and yields the thermal properties of the sample on a micrometer scale, depending on sample parameters and modulation frequency. For the experiments reported here, we used modulation frequencies up to 7 MHz resulting in a spatial resolution of about 5 μm.

Micro-Raman/photoluminescence and infrared transmission investigations were performed at room temperature using a conventional Raman microspectroscopy triple system (ISA T64000) and a conventional Fourier transform IR spectrometer (Bruker IFS 66), respectively. The Raman/luminescence spectra were obtained at a laser wavelength of 488 nm with a focal diameter of about 1 μm. Confocal imaging yields surface-sensitive Raman/luminescence signals. The infrared microscope enables a spot diameter of about 20 μm.

3. Results and discussion

In order to visualize the microscopic structure of the polished growth surface of the CVD sample investigated, transmission light microscopy was used. The transmission light microscope image of the sample is shown in Fig. 1. The sample exhibits statistically oriented grains with an average size of 28 μm at the growth surface. Owing to the scattering and absorption of the transmitted light, the defective regions located between the crystallites appear larger in comparison with its real dimensions. These defective regions can be either grain boundaries or microcracks, which would both be expected to be ideal accumulation areas for impurities. The microscopic thermal and optical mapping was carried out along the line indicated in Fig. 1. Starting and end points of the mapping experiments, as well as the dominant visible defective region, are labelled by their distances from the sample edge.

In Fig. 2 the thermal diffusivity values obtained by mapping (indicated by the line in Fig. 1) over crystallites and regions located between crystallites at the growth surface of the sample at room temperature are plotted versus the distance from the sample edge. The grating period of = 63 μm yields a spatial resolution of about 20 μm. The main feature of the results is a significant decrease in the diffusivity of about 35% at 420 μm, which can be attributed to a clearly visible defective region located between crystallites at this position. After this significant reduction in the diffusivity, it increases

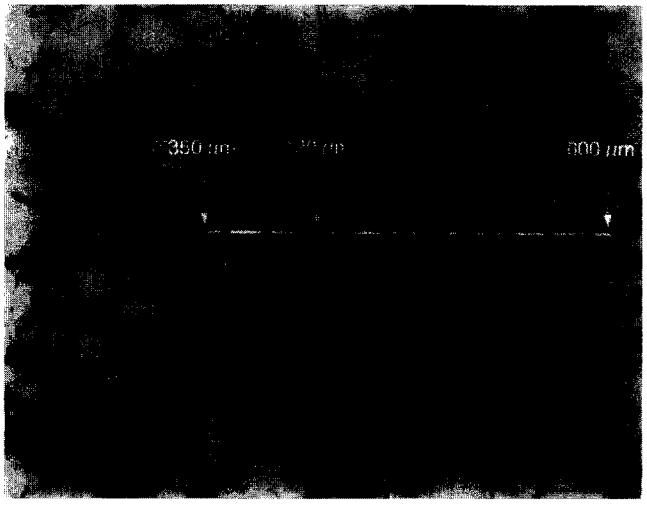

Fig. 1. Transmission light microscope image of the CVD diamond film investigated. The thermal and optical mapping experiments were carried out along the broken line. Selected positions along this line are indicated.

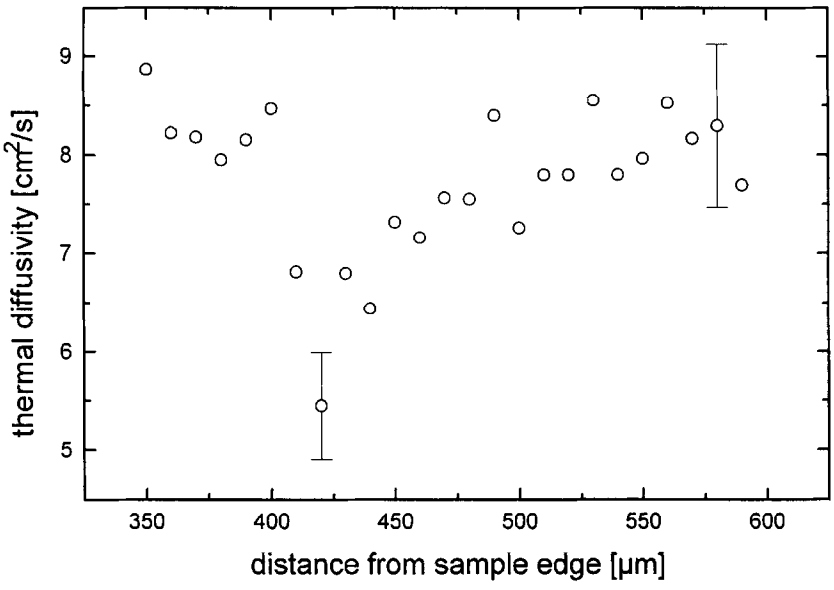

Fig. 2. Thermal diffusivities obtained by mapping along the line indicated in Fig. 1 using the photothermal displacement technique at transient thermal gratings with a grating period of $\Lambda = 63$ μm.

continuously up to values which are comparable with the starting region between 350 and 400 μm. In this region consisting of two large crystallites, thermal diffusivity values of about 8.3 $cm^2\ s^{-1}$ were measured, which is equivalent to a thermal conductivity of 1500 W $m^{-1}K^{-1}$.

Fig. 3 shows the signal amplitude recorded with the photothermal microscope. This amplitude is proportional to the surface temperature at the point being measured. Similarly to the transient thermal grating measurement, a significant rise of the signal at 420 μm occurs, indicating an obstacle to the heat flow. Additionally, the photothermal signal exhibits some smaller structures revealing weak but detectable thermal barriers induced by defective regions located between

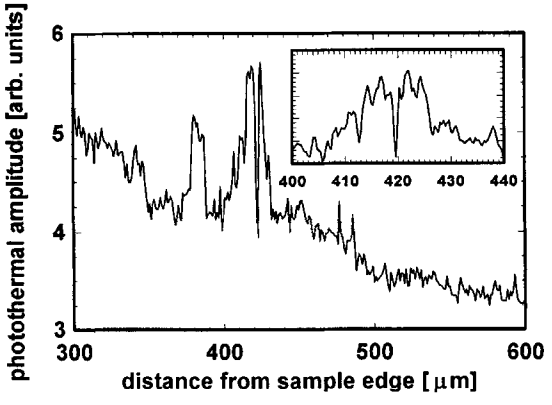

Fig. 3. Signal recorded with the photothermal microscope along the line indicated in Fig. 1. Pump and probe beam were focused on the same spot. The modulation frequency was 7 MHz and the pump beam intensity was 50 mW. The insert shows a more detailed measurement of the vicinity of the feature at 420 μm.

crystallites. The vicinity of the significant feature corresponding to a thermal barrier induced by the dominant defective region at 420 μm was further investigated in detail and the results are shown as an insert in Fig. 3. On both sides of the thermal barrier, the temperature increases because of reflection of the thermal waves at the barrier. In the case of a barrier dimension narrow compared with the spatial resolution, the situation just above the barrier is nearly symmetric and no reflection of the thermal waves occurs, yielding a significant temperature dip. An extension of an analytical theory [6] with slightly modified boundary conditions yields a thermal conductivity of 1700 W $m^{-1}K^{-1}$ in the crystallites on both sides of the defective region and a thermal resistance of 8.5×10^{-9} $m^2K\ W^{-1}$ across the defective region.

In order to directly compare the observed thermal diffusivity behaviour with the incorporation of different defect types, we repeated the mapping in an identical manner with micro-Raman, micro-photoluminescence and infrared spectroscopy; the results are shown in Fig. 4. The Raman G-peak typically centered at 1570 cm^{-1} is related to non-diamond carbon. Phonon-coupled luminescence bands with zero-phonon lines at 1.681 and 2.156 eV can be attributed to silicon-vacancy and nitrogen-vacancy complexes, respectively [7,8]. For eliminating the influence of the scattering volume and enabling a semiquantitative analysis, the integrated zero-phonon line and G-peak intensities were normalized to the integrated diamond Raman line intensity. The infrared broad absorbance bands between 2800 and 3000 cm^{-1} are related to C–H stretch modes. In Fig. 4, the normalized Raman/luminescence intensities and integrated

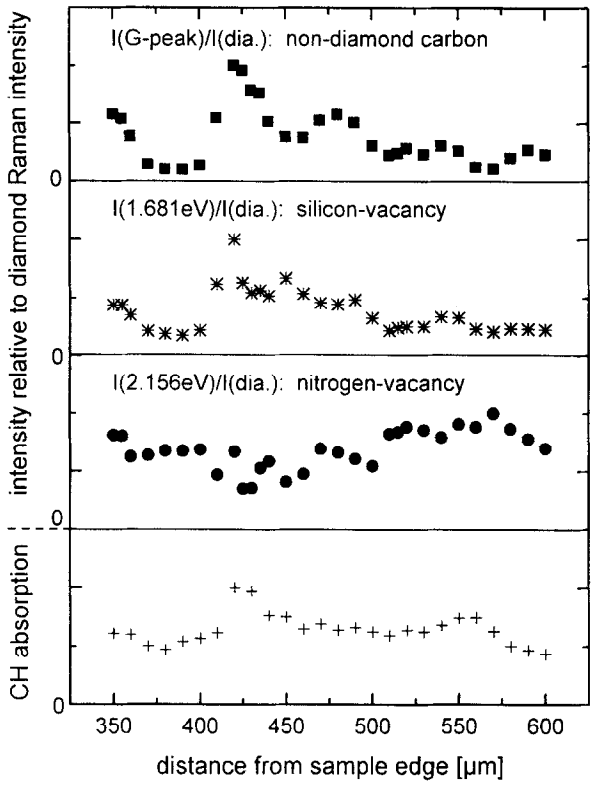

Fig. 4. Defect intensities obtained by mapping along the line indicated in Fig. 1 using Raman, luminescence and infrared spectroscopy. The intensities of the Raman G-peak and luminescence lines were normalized to the diamond Raman line intensity. The normalized Raman/luminescence intensities and CH-absorption were scaled differently for better clarity.

CH–absorption are plotted versus the distance from the sample edge and were scaled differently for better clarity. At the position of the dominant defective region at 420 μm the normalized G-peak and 1.681 eV luminescence intensities exhibit sharp maxima. The integrated CH absorption has its main maximum at the same position. After this sharp rise, these defect intensities show a decreasing tendency in correlation with the observed improvement of the thermal properties to be recognized in Fig. 2. Owing to the high lateral resolution of the Raman/luminescence measurements of about 1 μm, the normalized G-peak and 1.681 eV luminescence intensities exhibit a fine structure with a number of additional weaker maxima. For example, the maxima at 350 μm can likewise be related to the edge of the visible defective region located between crystallites seen in Fig. 1 at the starting point of the mapping line. In contrast to the other defects investigated, nitrogen-vacancy complexes are homogeneously incorporated in the film as the normalized 2.156 eV luminescence indicates. Therefore, the significant decrease in the thermal diffusivity at 420 μm is correlated with a preferential incorporation of non-diamond carbon, silicon-vacancy complexes and hydrogen at this region.

Depending upon whether the defective region at 420 μm is a grain boundary or a microcrack located within the probing depths of the measurement methods used (5 – 20 μm) near the growth surface, the correlation between the microscopic thermal and optical spectroscopy data can be discussed differently. Both grain boundaries and microcracks are ideal accumulation areas for defects. The results of the optical spectroscopy mapping experiments suggest that these defects are clusters of non-diamond carbon passivated with hydrogen, clusters of segregated hydrogen and silicon-vacancy complexes. Should the defective region at 420 μm be a grain boundary, the thermal diffusivity is reduced due to enhanced phonon scattering from these defects, which are preferentially incorporated in the vicinity of this grain boundary. A concentration of defects near grain boundaries is suggested by transmission electron microscopy [9], and recent research demonstrates that hydrogen is mostly incorporated in noncrystalline and defective regions at grain boundaries or dislocations of CVD diamond films [10]. If the defective region at 420 μm is a microcrack, the transmission probability of phonons across the crack drops significantly even if the thickness of the crack is only a few interatomic spacings and thus, the thermal diffusivity will be degraded. In this case the concentration of defects at the microcrack is only a side effect, which would not cause the decrease in the thermal diffusivity. Recent publications have discussed the role of microcracks between crystallites with regard to the thermal conductivity of polycrystalline diamond films [11,12]. Comparing Fig. 1 with the results of the microscopic mapping experiments, it must be pointed out that several grain boundaries crossing the mapping line have no significant deleterious effect on the thermal properties, because these boundaries only exhibit weak or no accumulation of defects. Thus, the experiments reported here reveal that regions located between crystallites can have different qualities with respect to defect incorporation and the induction of thermal barriers, whereas both the transient thermal grating technique and the photothermal microscopy determined high thermal conductivities within the crystallites at room temperature (1500 – 1700 $W\,m^{-1}K^{-1}$). Further systematic work on a micrometer scale is required in order to explore the relation of the thermal properties of polycrystalline diamond films to its microscopic structure and the distinct microscopic phonon scattering mechanisms.

4. Conclusions

In summary, we reported on mapping experiments on a micrometer scale, using photothermal and optical spectroscopy methods, in order to relate the thermal properties and the incorporation of defects to the micro-

scopic structure of CVD diamond. The thermal diffusivity is reduced up to 35 % in a defective region located between crystallites, in correlation with the preferential incorporation of non-diamond carbon, silicon-vacancy complexes and hydrogen at this region. This correlation can be understood either in terms of enhanced phonon scattering from these defects accumulated at a grain boundary or in terms of a significant drop of the transmission probability of phonons caused by a defect-filled microcrack located at this region. Differences in the quality of regions located between crystallites with respect to defect incorporation and the induction of thermal barriers were observed. High thermal conductivity values between 1500 W $m^{-1}K^{-1}$ and 1700 W $m^{-1}K^{-1}$ were determined within the crystallites at room temperature.

Acknowledgments

The authors wish to thank O.W. Käding and K.E. Goodson for valuable discussions.

References

[1] K.E. Goodson, O.W. Käding, M. Rösler, R. Zachai, *J. Appl. Phys., 77* (1995) 1385.
[2] K.E. Goodson, O.W. Käding, R. Zachai, *1994 ASME Winter Annual Meeting,* Chicago, IL, November 11–18.
[3] O.W. Käding, H. Skurk, A.A. Maznev, E. Matthias, *Appl. Phys. A, 61* (1995) 253.
[4] O.W. Käding, M. Rösler, R. Zachai, H.-J. Füßer, E. Matthias; *Diamond and Relat. Mater., 3* (1994) 1178.
[5] J. Opsal, A. Rosencwaig, D.L. Willenborg, *Appl. Opt., 22* (1983) 3169.
[6] M. Reichling, H. Grönbeck, *J. Appl. Phys., 75* (1994) 1914.
[7] A.T. Collins, L. Allers, C.J.H. Wort, G.A. Scarsbrook, *Diamond and Relat. Mater., 3* (1994) 932.
[8] L.H. Robins, D.R. Black, *J. Mater. Res., 9* (1994) 1298.
[9] A.V. Hetherington, C.J.H. Wort, P. Southworth, *J. Mater. Res., 5* (1990) 1591
[10] B. Dischler, C. Wild, W. Müller-Sebert, P. Koidl, *Physica B, 185* (1993) 217.
[11] J.E. Graebner, M.E. Reiss, L. Seibles, T.M. Hartnett, R.P. Miller, C.J. Robinson, *Phys. Rev. B, 50* (1994) 3702.
[12] K.M. McNamara Rutledge, B.E. Scruggs, K.K. Gleason, *J. Appl. Phys., 77* (1995) 1459.